Axitinib blocks Wnt/β-catenin signaling and directs asymmetric cell division in cancer

Yi Qu[a,b], Naouel Gharbi[c], Xing Yuan[d], Jan Roger Olsen[a], Pernille Blicher[e], Bjørn Dalhus[e,f], Karl A. Brokstad[a,g], Biaoyang Lin[h], Anne Margrete Øyan[a], Weidong Zhang[d], Karl-Henning Kalland[a,b,i,1], and Xisong Ke[a,1]

[a]Department of Clinical Science, University of Bergen, N-5021 Bergen, Norway; [b]Department of Microbiology, Haukeland University Hospital, N-5021 Bergen, Norway; [c]Institute of Marine Biology, University of Bergen, N-5020 Bergen, Norway; [d]Department of Phytochemistry, College of Pharmacy, Second Military Medical University, Shanghai 200433, People's Republic of China; [e]Department of Medical Biochemistry, Institute for Clinical Medicine, University of Oslo, N-0424 Oslo, Norway; [f]Department of Microbiology, Oslo University Hospital HF, Rikshospitalet, N-0424 Oslo, Norway; [g]Broegelmann Research Laboratory, Department of Clinical Science, University of Bergen, N-5021 Bergen, Norway; [h]Collaborative Innovation Center for Diagnosis and Treatment of Infectious Diseases, The First Affiliated Hospital, School of Medicine, Zhejiang University, Hangzhou, 310003 People's Republic of China; and [i]Centre for Cancer Biomarkers, University of Bergen, N-5021 Bergen, Norway

Edited by Dennis A. Carson, University of California, San Diego, La Jolla, CA, and approved June 27, 2016 (received for review March 18, 2016)

Oncogenic mutations of the Wnt (wingless)/β-catenin pathway are frequently observed in major cancer types. Thus far, however, no therapeutic agent targeting Wnt/β-catenin signaling is available for clinical use. Here we demonstrate that axitinib, a clinically approved drug, strikingly blocks Wnt/β-catenin signaling in cancer cells, zebrafish, and $Apc^{min/+}$ mice. Notably, axitinib dramatically induces Wnt asymmetry and nonrandom DNA segregation in cancer cells by promoting nuclear β-catenin degradation independent of the GSK3β (glycogen synthase kinase3β)/APC (adenomatous polyposis coli) complex. Using a DARTS (drug affinity-responsive target stability) assay coupled to 2D-DIGE (2D difference in gel electrophoresis) and mass spectrometry, we have identified the E3 ubiquitin ligase SHPRH (SNF2, histone-linker, PHD and RING finger domain-containing helicase) as the direct target of axitinib in blocking Wnt/β-catenin signaling. Treatment with axitinib stabilizes SHPRH and thereby increases the ubiquitination and degradation of β-catenin. Our findings suggest a previously unreported mechanism of nuclear β-catenin regulation and indicate that axitinib, a clinically approved drug, would provide therapeutic benefits for cancer patients with aberrant nuclear β-catenin activation.

axitinib | β-catenin | asymmetric cell division | SHPRH

WNT (wingless)/β-catenin signaling is an evolutionarily conserved pathway and is essential for development in nearly all tissues and organ systems. In adulthood, WNT/β-catenin signaling is required for adult stem cells (ASCs) to maintain tissue homeostasis, regeneration, and injury repair (1). In the signaling cascade, a key step is the degradation of β-catenin by the Axin/GSK3β (glycogen synthase kinase 3β)/APC (adenomatous polyposis coli) destruction complex (2). Cancer genome sequencing has revealed frequent mutations of *APC* and *CTNNB1* (*catenin beta 1*) in major tumors, and most of these mutations are predicted to result in aberrant activation of WNT/β-catenin signaling.

During the last decade, a number of Wnt inhibitors have been reported; however, only a few have moved to phase I or phase II clinical trials (1), possibly because of the general obstacles inherent in new drug development; this impediment can be avoided by the identification of novel therapeutic targets of already approved drugs with well-characterized bioactivity and safety profiles. Another possible problem is that many of these inhibitors target the Wnt signaling at or upstream of the Axin/GSK3β destruction complex, whereas most of the Wnt pathway mutations (*APC* and *CTNNB1*) in cancer patients are downstream of that level. For therapeutic purposes, it is critical to develop drugs targeting downstream of the destruction complex, ideally at the end of the pathway.

A major challenge in targeting Wnt/β-catenin signaling is to distinguish cancer cells from the long-term repopulating ASCs required for maintaining tissue homeostasis (3). It has been supposed that a fundamental difference between them is the type of cell division: ASCs divide asymmetrically under steady-state conditions to maintain population size and tissue homeostasis, whereas symmetric division is advantageous for neoplastic transformation and excessive expansion of malignant cells leading to uncontrolled tumor growth (4, 5). Emerging evidence indicates the critical role of defective asymmetric division in tumor initiation and progression (5). In particular, the loss of asymmetric division contributes to the oncogenic role of mutant APC in hyperplasia and tumorigenesis as well as in the activation of Wnt/β-catenin signaling (6). Therefore, forcing a switch from symmetric to asymmetric division in cancer cells could allow cancer therapy without damaging normal tissue homeostasis.

Our goal was to discover clinically approved drugs that block Wnt/β-catenin signaling downstream of the destruction complex. We supposed that desirable drugs would be able to inhibit Wnt signaling stimulated by GSK3β inhibitor and mutant β-catenin. To visualize Wnt inhibition, we used fluorescent reporters to monitor the Wnt/β-catenin activity upon drug treatment in vitro and in vivo. Finally, chemo-proteomic approaches were used for global and unbiased identification of the target proteins of the Wnt inhibitor.

Significance

The Wnt (wingless)/β-catenin signaling pathway is an attractive target for cancer therapy. However, known Wnt inhibitors are still far from clinical use. Here we report that the clinically approved drug axitinib strongly inhibits Wnt/β-catenin signaling in vitro and in vivo. In particular, a phenotype of Wnt inhibition called "Wnt asymmetry" was revealed in axitinib-treated cancer cells. The identification of E3 ubiquitin ligase SHPRH (SNF2, histone-linker, PHD and RING finger domain-containing helicase) as the functional target implies that axitinib blocking of Wnt signaling is independent of genetic mutations that are frequently observed in cancer patients. Collectively, our results suggest a mechanism of nuclear β-catenin regulation and highlight axitinib as a promising therapeutic agent for cancer patients with aberrant Wnt/β-catenin signaling.

Author contributions: Y.Q., K.-H.K., and X.K. designed research; Y.Q., N.G., X.Y., J.R.O., P.B., B.D., K.A.B., A.M.Ø., W.Z., and X.K. performed research; Y.Q., N.G., B.L., K.-H.K., and X.K. analyzed data; and Y.Q., N.G., B.D., K.-H.K., and X.K. wrote the paper.

Conflict of interest statement: The Technology Transfer Organization of University of Bergen (BTO) has filed a patent application (pending) for the use of axitinib as a WNT/β-catenin inhibitor in selected cancer types. None of the authors are affiliated with BTO. X.K., Y.Q., K.-H.K., and A.M.Ø are the inventors of the patent.

This article is a PNAS Direct Submission.

Data deposition: The DNA microarray data reported in this paper have been deposited in the ArrayExpress database (accession nos. E-MTAB-3438 and E-MTAB-3652).

[1]To whom correspondence may be addressed. Email: Xisong.Ke@uib.no or Kalland@uib.no.

This article contains supporting information online at www.pnas.org/lookup/suppl/doi:10.1073/pnas.1604520113/-/DCSupplemental.

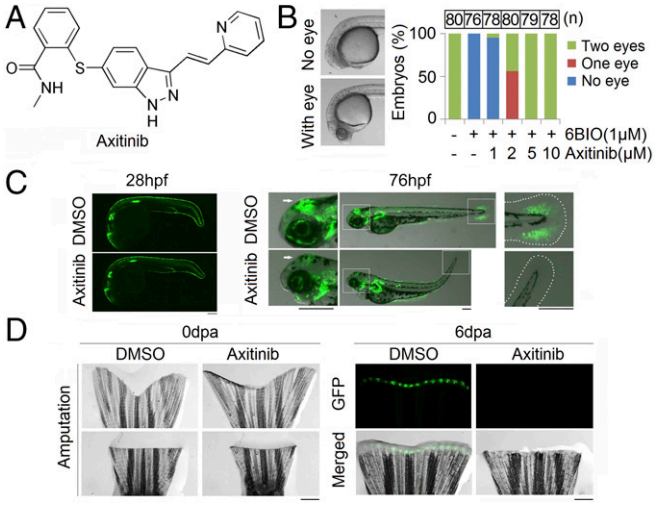

Fig. 1. Axitinib inhibits Wnt/β-catenin signaling in zebrafish. (*A*) Chemical structure of axitinib. (*B*) Zebrafish embryos at 6 h post fertilization (hpf) were treated with 6BIO and axitinib at the indicated concentrations, and the eyeless phenotype was assessed 24 h later. n = total number of assessed embryos over four independent experiments. Embryos that died during treatment (n = 0, 4, 2, 0, 1, and 2 in the groups from left to right) were excluded from assessment. (*C*, *Left*) Representative images at 28 hpf of TCF-GFP transgenic zebrafish embryos treated with DMSO or axitinib (5 μM) for 2 d. n = 40 in each group; no embryos died. (*Right*) Representative images at 76 days post fertilization (dpf). The middle–hindbrain boundary (white arrows) and caudal fin mesenchyme are enlarged at the left and right, respectively. (*D*) Representative images of tailfin regeneration in TCF-GFP transgenic zebrafish (13 wk, n = 5 fish per group) treated with DMSO or axitinib (5 μM) for 6 d post amputation (dpa). Scale bars, 200 μm.

Results

Axitinib Targets Wnt/β-Catenin Signaling in Vitro and in Vivo. To target Wnt/β-catenin signaling downstream of the destruction complex, we used a specific GSK3 inhibitor, 6-bromoindirubin-3′-oxime (6BIO), to activate Wnt signaling (7) (Fig. S1 *A* and *B*). In a screen of 460 Food and Drug Administration (FDA)-approved drugs, axitinib showed the strongest inhibition of 6BIO-stimulated TOPFlash activity (Fig. 1*A* and Fig. S1 *C*–*E*). To visualize Wnt inhibition, we used a lentiviral Wnt 7TGC reporter containing a T-cell factor (TCF) promoter driving GFP and a SV40 promoter driving mCherry (Fig. S1*F*) (8). In prostate EPT1 cells, TCF-GFP was silenced but was strongly activated by 6BIO, and this GFP activation was significantly blocked by additional treatment with axitinib (Fig. S1*G*). A similar observation was obtained in EPT1 cells harboring a 7TC (TCF-mCherry) reporter derived from 7TGC (Fig. S1 *F* and *G*). Axitinib also blocked the Wnt signaling in 293FT cells overexpressing mutated β-catenin lacking the N-terminus (ΔN47) or with mutations at Ser33A/Ser37A/Thr41A/Ser45A (4A), which are resistant to GSK3β phosphorylation-mediated degradation (Fig. S1*H*).

In zebrafish embryos, abnormal activation of Wnt/β-catenin signaling generates an eyeless phenotype (9). As predicted, 6BIO at 1 μM readily induced the loss of eyes in all the treated embryos, but this eyeless phenotype was dose-dependently and totally rescued by cotreatment with axitinib (Fig. 1*B*). In transgenic zebrafish carrying a Wnt reporter TCF-GFP (10), embryos exposed to axitinib for 3 d showed significantly shorter body length and thinner tails as well as a decrease in TCF-GFP expression in the midbrain–hindbrain boundary and in fin mesenchymal cells where Wnt signals are required during development (Fig. 1*C*) (11, 12).

Axitinib Blocks Wnt Signaling in Cancer and Tissue Regeneration. Colon cancer SW480, HCT116, and RKO cells harbor mutant *APC* (Wnt activated), *CTNNB1* (Wnt activated), and neither mutation (Wnt inactivated), respectively (Fig. S2*A*). As expected, the TOPFlash activities in SW480 and HCT116 cells were significantly repressed by axitinib treatment (Fig. S2*B*). In SW480-7TGC cells, axitinib dose-dependently increased the proportion of TCF-GFP^{low} cells (Fig. S2 *C* and *D*). Notably, most of these TCF-GFP^{low} cells were induced to apoptosis, as marked by high Hoechst labeling, because of chromatin condensation and fragmentation (Fig. S2*D*). In soft agar assay, colonies formed in SW480 and HCT116 cells but not in RKO cells, suggesting that colony formation of colon cancer cells is dependent on Wnt/β-catenin signaling (Fig. S2*E*). Significantly, axitinib strongly and dose-dependently inhibited colony growth of both SW480 and HCT116 cells (Fig. S2*E*). Profiling gene expression in axitinib-treated SW480 cells revealed that 7 of the top 10 repressed genes are direct targets of Wnt (Fig. S2*F*) (13). Examination of the entire list of genes that are direct Wnt targets revealed that more than 25% were significantly repressed by axitinib, but none was upregulated (Fig. S2 *G* and *H*), indicating that axitinib-repressed genes in SW480 cells have a Wnt/β-catenin signaling signature.

Apc$^{min/+}$ mice spontaneously generate adenomas because of mutant *Apc*. The strong increase of β-catenin in all the adenomas demonstrates that Wnt/β-catenin signaling is highly relevant to tumor initiation and expansion in *Apc*$^{min/+}$ mice (Fig. S3*A*). Treatment with axitinib at 50 mg/kg daily for 5 wk significantly decreased the number of both multivillus adenomas and microadenomas in the small intestine (Fig. S3*B*). Importantly, obviously less and weaker staining of the proliferation marker Ki67 was found in axitinib-treated adenomas (Fig. S3*C*). We also tested axitinib in *Apc*-deleted murine organoids that grow independently of R-spondin because of β-catenin activation (14). Consistently, axitinib strongly inhibited the growth of Apc-mutant organoids (Fig. S3*D*).

Wnt/β-catenin signaling is required to maintain crypt integrity and intestinal homeostasis (15). Unexpectedly, no obvious change in mucosa organization or crypt size and density was found in the normal small intestine of axitinib-treated mice (Fig. S3*E*). In contrast to the decrease of Ki67 in adenomas, comparable regular and uniform distribution of Ki67^{+} cells was found in axitinib-treated normal intestine (Fig. S3*E*). In adult transgenic zebrafish, it has been established that Wnt/β-catenin signaling is activated by tailfin resection (16). Strikingly, the tailfin regrowth and TCF-GFP activation were completely inhibited in all fish treated with axitinib at 5 μM for six consecutive days (Fig. 1*D*). However, the regular and uniform incorporation of the mitotic marker BrdU in the crypts suggests the normal proliferative status of axitinib-treated intestine (Fig. S3*F*). Collectively, these data support the idea that axitinib strongly inhibits Wnt signaling in tumor growth and tissue regeneration with minor effect on adult tissue homeostasis.

Axitinib Directs Asymmetric Cell Division. We hypothesized that axitinib affects cell division because cell division is largely symmetric, leading to uncontrolled growth in tumor and to tissue repair in resected tailfin, whereas it is mainly asymmetric, maintaining tissue homeostasis, in normal intestine (4, 17). To assess cell division, SW480-7TGC cells were synchronized and plated singly before drug treatment. Fluorescence imaging revealed that up to 10% of axitinib-treated paired cells showed unequal TCF-GFP expression, but this unequal expression was never found in DMSO-treated control cells (Fig. 2*A*), suggesting a switch from symmetric cell division (SCD) to asymmetric cell division (ACD) in terms of Wnt signaling activity. Live-cell imaging indicates that paired cells with unequal Wnt signals are derived from single cells (Fig. S4*A*). This phenomenon, which we called "Wnt ACD," was examined further in prostate cancer EPT3-7TGC cells with low Wnt signaling. Consistently, Wnt ACD was readily found in paired cells cotreated with 6BIO and axitinib but never in cells treated with 6BIO alone (Fig. S4*B*). Wnt ACD also was observed in SW480-7TC cells in which TCF-mCherry marks Wnt activity (Fig. S4*C*). To characterize Wnt ACD functionally, we examined the proliferation marker Ki67 in SW480-7TC cells. Consistent with the induction of apoptosis in

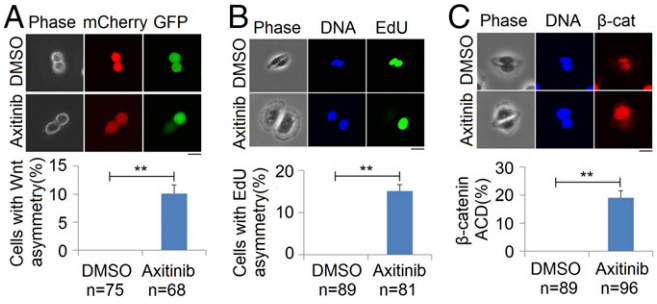

Fig. 2. Axitinib directs ACD. Microscope images and quantitation of paired cells treated with DMSO or 5 μM axitinib. (*A*) SW480-7TGC cells were treated for 24 h to detect TCF-GFP expression. (*B*) SW480 cells were treated for 72 h for the EdU label-release assay. (*C*) SW480 cells were treated for 24 h for β-catenin (β-cat) staining. $^{**}P < 0.01$. *n* = total paired counted cells over three independent experiments. Scale bars, 20 μm.

TCF-GFP^{low} cells (Fig. S2*D*), less frequent and less intense Ki67 staining was observed in TCF-mCherry^{low} cells (Fig. S5*A*), further indicating that proliferation in SW480 cells is dependent on Wnt signaling.

The observation of Wnt ACD encouraged us to assess nonrandom DNA segregation that is a well-established feature in stem cell ACD (18). We examined the chromosome segregation in axitinib-treated SW480 cells using an EdU (5-ethynyl-2'-deoxyuridine) label-release assay in which only newly synthesized DNA is labeled during cell division (Fig. S4*D*). Dramatically, around 15% of the paired cells exhibited unequal EdU labeling (EdU ACD), which was never found in control cells (Fig. 2*B*). EdU ACD was absent in HCT116 cells with activated Wnt signaling and in RKO cells with silenced Wnt signaling but increased significantly in axitinib-treated HCT116 cells (Fig. S4*E*). In RKO cells, pretreatment with 6BIO was required for EdU ACD induction by axitinib (Fig. S4*E*), indicating that axitinib-induced nonrandom DNA segregation is dependent on the inhibition of Wnt signaling.

Axitinib-induced ACD is further supported by immunofluorescence staining of β-catenin in axitinib-treated SW480 cells: Nearly 19% of paired cells displayed unequal distribution of nuclear β-catenin (β-catenin ACD) (Fig. 2*C*). To investigate the associations among EdU ACD, Wnt ACD, and β-catenin ACD, we performed EdU and β-catenin staining in SW480-7TC cells. Significantly, daughter cells with higher Wnt signaling preferably inherited the EdU-unlabeled DNA (Fig. S5*B*), and cells expressing higher levels of β-catenin exclusively showed stronger Wnt activity and frequently showed negative EdU staining (Fig. S5 *C* and *D*). The tight association between nonrandom DNA segregation and Wnt ACD implies cell-intrinsic reprogramming of SW480 cells by axitinib. Given that the loss of ACD is critical for tumor initiation and progression (4, 19, 20), the reestablishment of ACD in cancer cells by axitinib could potentially be a mechanism of tumor suppression.

Axitinib Promotes Nuclear β-Catenin Degradation Independent of GSK3β/APC. The observed β-catenin ACD raises the possibility that axitinib depletes nuclear β-catenin. Western blots confirmed the dose- and time-dependent decrease of β-catenin in axitinib-treated SW480 cells (Fig. S6*A*). In the presence of the proteasome inhibitor MG132, axitinib failed to reduce β-catenin but increased its ubiquitination (Fig. S6*B*). Additional treatment with the nuclear export inhibitor leptomycin B demonstrated the nuclear location of β-catenin degradation (Fig. S6*C*). Notably, reduced β-catenin also was observed in axitinib-treated murine adenomas (Fig. S6*D*). As expected, knockdown of β-catenin readily induced Wnt and EdU ACD (Fig. S6 *E* and *F*), indicating that axitinib directs ACD by promoting the degradation of nuclear β-catenin.

The N-terminal residues Ser45/Thr41/Ser37/Ser33 of β-catenin are required for GSK3β phosphorylation and β-transducin repeats containing protein (β-TrCP) ubiquitination in the presence of APC (21). Mutations of these residues are predominant in cancer patients and are sufficient to induce tumorigenesis (22). In *APC* mutant SW480 cells axitinib reduced the non-phospho (active) β-catenin (Ser33/37/Thr41) (ABC), GSK3β phospho-β-catenin (Ser33/Ser37/Thr41), CK1 phospho-β-catenin (Ser45), and β-catenin-4A with mutations in Ser45/Thr41/Ser37/Ser33 (Fig. S6 *G* and *J*), indicating that GSK3β, APC, and β-TrCP are not involved in axitinib-promoted β-catenin degradation. In contrast, the tankyrase inhibitor IWR1 promotes β-catenin degradation by stabilizing Axin but does not reduce the total β-catenin in *APC* mutant DLD cells (23). Of note, the tankyrase inhibitor XAV939 depletes total β-catenin in SW480 cells (24). In the present study, both tankyrase inhibitors decreased wild-type β-catenin but not the N-terminal mutant β-catenin in 293FT cells (Fig. S6*H*) and failed to reduce total β-catenin significantly or to induce Wnt ACD in SW480 cells (Fig. S6 *H* and *I*). Our data support the notion that in *APC*-truncated cells (e.g., SW480 cells) the Axin-bound β-catenin fails to be ubiquitinated and degraded (21). Independent of GSK3β and β-TrCP, β-catenin can be degraded by the E3 ubiquitin ligase TRIM33 that targets phosphorylated Ser715 or the autophagy protein LC3 that targets residues W504/I507 (25, 26). Both possibilities were ruled out because axitinib reduced β-catenin with mutations of all these residues (Fig. S6*J*), suggesting that an undescribed mechanism of axitinib induces β-catenin degradation.

Identification of the Proteins Directly Binding Axitinib. Axitinib is a known inhibitor of multireceptor tyrosine kinases, especially vascular endothelial growth factor receptors (VEGFRs) (Fig. S7*A*) (27). However, all the established tyrosine receptor kinase targets are silenced in SW480 cells (Fig. S7*B*). In addition, three other VEGFR inhibitors did not show Wnt inhibition (Fig. S7 *C* and *D*). Importantly, the loss of VEGFR1 does not reduce β-catenin, and VEGFR inhibitors block the regenerative angiogenesis but not tailfin regrowth in zebrafish (28, 29), suggesting that axitinib inhibits Wnt signaling independently of VEGFRs in vitro and in vivo.

To identify the proteins that bind directly to axitinib, we used a label-free small-molecule target-identification strategy called "DARTS" (drug affinity-responsive target stability), in which the potential target proteins are stabilized by binding to small molecules and thus can be protected and enriched following proteolysis (30). After pronase proteolysis, SW480 DARTS samples were resolved in 2D-DIGE (2D difference in gel electrophoresis); 11 spots appeared, with strikingly differential intensities; all were stronger in axitinib-treated samples (Fig. 3*A* and Fig. S8 *A*–*C*), supporting the strategy of protecting protein targets by binding to small molecules. Mass spectrometry analysis of these spots identified a number of proteins (Fig. S8*D*). As is consistent with the results shown in Fig. S7*B*, no receptor tyrosine kinase was detected in these spots.

Considering that axitinib inhibits Wnt signaling by promoting nuclear β-catenin turnover, proteins with nuclear localization and activities connected with protein degradation were prioritized for follow-up. According to the literature, SHPRH (SNF2, histone-linker, PHD and RING finger domain-containing helicase), MYCBP2, and BIRC6 are known ubiquitin ligases, but only SHPRH is well recognized as a nuclear protein that is critical for DNA repair (31).

Western blot analysis of the DARTS samples confirmed the mass spectrometry data and revealed the stabilization of SHPRH by axitinib at lower concentrations (Fig. S8*E*). Independent evaluation of the direct binding of axitinib and SHPRH was performed by microscale thermophoresis (MST), an all-optical

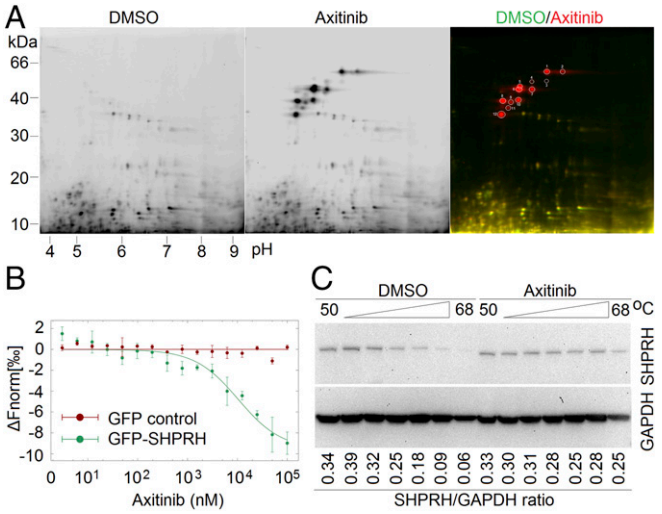

Fig. 3. Identification of proteins binding directly to axitinib. (*A*) 2D-DIGE images of the DARTS samples. SW480 protein lysates were incubated with axitinib (150 μM) or an equal volume of DMSO and were digested with pronase before 2D-DIGE. (*B*) MST analysis of axitinib binding to GFP-SHPRH (four replicates) or free GFP (negative control; two replicates) in SW480 cell lysates. The fitted binding curve gives a K_d of 10.4 ± 3.3 μM. (*C*) Western blots of intact cell CETSA samples. SW480 cells were incubated with axitinib (10 μM) or an equal volume of DMSO for 2 h at 37 °C followed by heating at the indicated temperatures. Cells were lysed, and the soluble portion was analyzed using Western blot. The abundance of SHPRH normalized to GAPDH is shown.

approach measuring the directed motion of GFP-tagged proteins in temperature gradients (32, 33). SW480 cell lysates containing GFP-tagged SHPRH or free GFP as a control were incubated with axitinib briefly (less than 1 min) before MST assay. As expected, a robust binding curve was observed in the GFP-SHPRH sample with a K_d at 10.4 ± 3.3 μM (Fig. 3*B*). Of note, in another experiment the K_d value of human interferon gamma and the antibody determined by MST was 16 times higher in cell lysates than PBS buffer (32, 33), implying that the K_d of axitinib and purified SHPRH could be at the nanomole level. In addition, axitinib at 10 μM significantly increased the stability of SHPRH in an intact living cell-based cellular thermal shift assay (CETSA) assay (Fig. 3*C*) (34), supporting the physical interaction of axitinib with SHPRH in vivo.

SHPRH Is Required for Axitinib-Induced β-Catenin Degradation. Given that SHPRH is an E3 ubiquitin ligase (31), we hypothesized that SHPRH is involved in axitinib-induced β-catenin ubiquitination and degradation. Indeed, in SW480 cells transfected with GFP-tagged SHPRH, obviously lower β-catenin expression was observed in cells overexpressing SHPRH (Fig. 4*A*). Western blotting confirmed that, similar to axitinib treatment, SHPRH reduced not only endogenous β-catenin but also β-catenin with the 4A or ΔN47 mutations or lacking the C terminus (ΔC) (Fig. 4*B* and Fig. S9*A*). In a dose–course experiment, a clear decrease in β-catenin was observed when the GFP-SHPRH was three times higher than endogenous SHPRH (Fig. S9*B*). To test the ubiquitin ligase dependence, we created catalytically inactive SHPRH by replacing the conserved cysteine 1432 in the RING domain to alanine (C1432A) (35). As expected, much less decrease in β-catenin was observed in SW480 cells overexpressing mutant SHPRH (Fig. 4*C*). When cells were treated with the proteasome inhibitor MG132, wild-type but not mutant SHPRH strongly increased the ubiquitination level of β-catenin (Fig. 4*C*).

The same readout of β-catenin turnover suggests that axitinib positively regulates SHPRH. The simplest explanation for the mechanism could be that axitinib increases SHPRH expression. Examination of the DNA microarray data did not find any change in SHPRH mRNA in axitinib-treated cells. However, in the presence of the protein biosynthesis inhibitor cycloheximide, treatment with axitinib clearly increased the half-life of SHPRH (Fig. S9*C*), suggesting that axitinib positively regulates SHPRH protein stability. To assess the role of SHPRH in axitinib-induced β-catenin degradation, we depleted SHPRH in SW480 cells by siRNAs (Fig. S9*D*). As expected, SHPRH knockdown not only increased the level of β-catenin protein but also blocked the axitinib-mediated decrease in β-catenin (Fig. 4*D*). Consistently, axitinib failed to increase the ubiquitination of β-catenin in SHPRH-knockdown cells (Fig. 4*E*). Collectively, these data demonstrate that SHPRH is required for axitinib's degradation of β-catenin.

SHPRH Negatively Regulates Wnt/β-Catenin Signaling. We further assessed the effect of SHPRH on Wnt signaling activity. In SW480 cells, TOPFlash activity was significantly repressed by overexpression of SHPRH (Fig. 5*A*). In SW480-7TC cells Wnt signaling is marked by TCF-mCherry expression, and transfection of GFP-tagged SHPRH clearly reduced TCF-mCherry expression (Fig. 5*B*). Notably, in SW480 cells stably overexpressing GFP-tagged SHPRH, unequal TCF-mCherry intensity was readily observed in paired cells (Fig. 5*C*), indicating that Wnt ACD also is induced by SHPRH. Interestingly, overexpression of SHPRH strongly inhibited the colony growth of SW480 cells (in which Wnt is activated) but not of RKO cells (in which Wnt is inactivated) (Fig. 5*D*). Of note, much

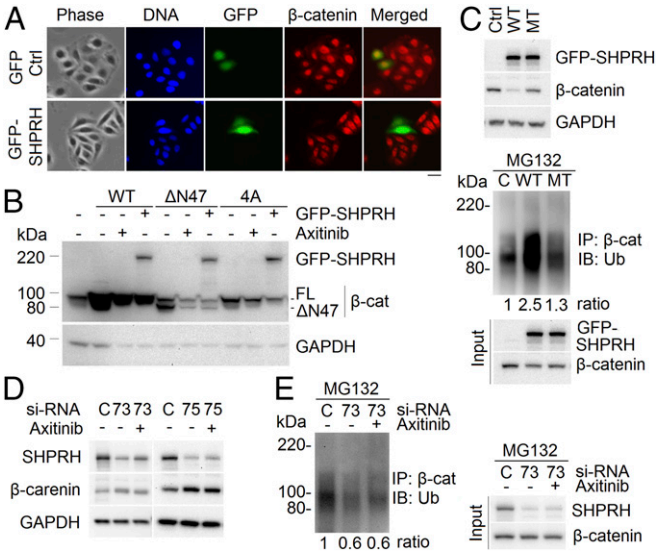

Fig. 4. SHPRH is required for axitinib degradation of β-catenin. (*A*) Representative β-catenin staining in SW480 cells transfected with GFP-tagged SHPRH or control GFP vector for 24 h. Endogenous β-catenin was reduced in cells overexpressing SHPRH. Experiments were performed in triplicate with high reproducibility. Scale bar, 20 μm. (*B*) Overexpression of GFP-SHPRH or axitinib treatment in SW480 cells reduced β-catenin in wild-type cells and in cells with the indicated mutations. FL, full length. (*C*) SHPRH increases the ubiquitination and turnover of β-catenin. SW480 cells were transfected with GFP (control, Ctrl) or with wild-type or mutant (MT) GFP-SHPRH for 24 h (*Upper*) and in addition were treated with MG132 (20 μM) for 6 h (*Lower*). C, control. (*D*) Western blots of SW480 cells transfected with siRNAs and treated with axitinib (5 μM) as indicated for 24 h. C, control; 73, si-SHPRH-73; 75, si-SHPRH-75. (*E*) Ubiquitination assay of β-catenin. SW480 cells were transfected with control (C) or SHPRH (73) siRNAs for 24 h and were treated with MG132 (20 μM) together with DMSO or axitinib (5 μM) for 6 h. The quantification of ubiquitylated β-catenin is shown in *C* and *E*.

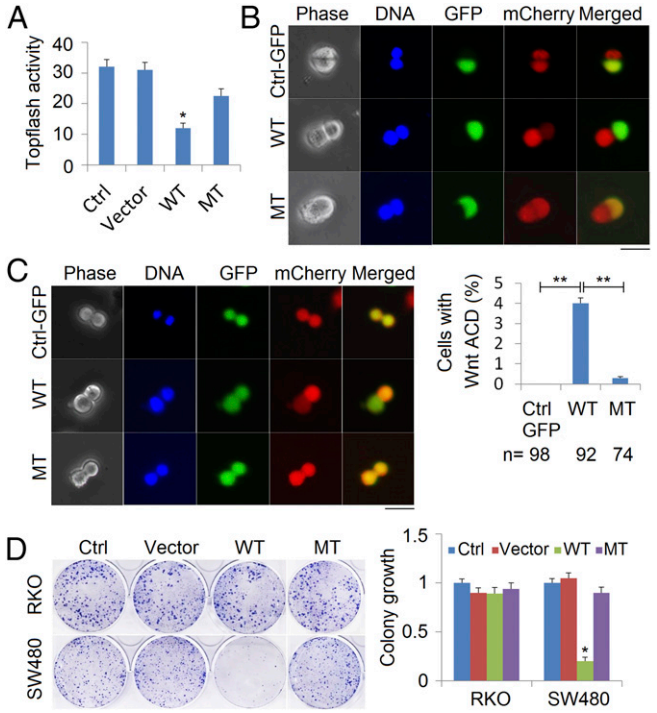

Fig. 5. SHPRH negatively regulates Wnt signaling. (*A*) TOPFlash assay of SW480 cells transfected with wild-type or mutant (MT) GFP-SHPRH, non-transfected control (control) or empty vector (vector). (*B*) Representative microscope images of TCF-mCherry expression in SW480-7TC cells transfected with the indicated vectors. Cells were seeded singly on new plates 24 h later, and images were captured after 10 h. In some dividing cells plasmids were lost cells during cell division. (*C*) SW480-7TC cells were transfected as indicated for 24 h and passaged twice in 6 d. Paired cells retaining plasmids (marked by GFP expression) in both daughter cells were imaged and scored for the TCF-mCherry expression. $^{**}P < 0.01$. Scale bar, 20 μm. (*D*) Representative images (*Left*) and quantification (*Right*) of colony formation in SW480 cells overexpressing wild-type or mutant (MT) SHPRH for 2 wk. Colony growth was quantified by measurement of OD_{590}. The graph presents the normalized OD_{590} ratios of experiments performed in triplicate. $^{*}P < 0.05$.

less Wnt inhibition, Wnt ACD, and colony growth inhibition were observed in SW480 cells overexpressing mutant SHPRH (Fig. 5).

Finally, we examined the SHPRH-affected transcription in SW480 cells by DNA microarrays. Comparison of the genes changed in SW480 cells with axitinib treatment and SHPRH transfection revealed a striking overlap (56%) of the top 400 repressed genes (Fig. S9*E*). Importantly, many of these commonly repressed genes, e.g., *AXIN2*, *NKD1*, and *LGR6*, are direct Wnt targets (Fig. S9*F*), further indicating that SHPRH is a functional target of axitinib in Wnt inhibition.

Discussion

Axitinib is a marketed VEGFR inhibitor used for treatment of renal cell carcinoma (27). In this study, we have demonstrated strong inhibition of Wnt/β-catenin signaling by axitinib independent of VEGFRs in vitro and in vivo, suggesting that the clinical use of axitinib might be expanded to cancer patients with aberrant nuclear β-catenin accumulation in tumor biopsies. The identification of SHPRH as the functional target of axitinib in blocking Wnt signaling and the identification of the newly reported target BCR-ABL1 (36) strongly support the notion that, although drugs are intended to be selective, many effective drugs bind to multiple molecules rather than to single targets, and this polypharmacology probably is therapeutically essential (37). Notably, another axitinib-binding protein, MED23, is also relevant to Wnt signaling (Fig. S8*D*); shRNA knockdown of MED23 in SW480 cells decreased TOPFlash activity but not the β-catenin level (Fig. S8 *F* and *G*), suggesting an alternative mechanism of Wnt inhibition.

Although the concentrations required to inhibit Wnt signaling and direct ACD in cultured cells are much higher than the approved (i.e., nanomole) potencies on the primary targets of axitinib (27), we did not observe significant toxicity of axitinib at 5 μM (the concentration required for Wnt inhibition) in Wnt-inactivated EPT1 and RKO cells. In fish embryos, the shorter body length and thinner tail could be explained by the inhibition of Wnt signaling (Fig. 1*C*). In adult fish (13 wk), no clear defect or morphology change was observed upon treatment with axitinib (5 μM) for 6 d (Fig. 1*D*). In $Apc^{Min/+}$ mice, axitinib inhibited intestinal adenoma growth and decreased the β-catenin at a dose (50 $mg{\cdot}kg^{-1}{\cdot}d^{-1}$) that is comparable to the ED_{70} dose (30 mg/kg, twice daily) required for the inhibition of VEGFR2 in mice (27). For therapeutic purposes, it will be important to evaluate Wnt inhibition in patient samples at the clinically used dose. On the other hand, axitinib at higher concentrations potentially targets more proteins; therefore it is necessary to examine the roles of other binding proteins in axitinib-mediated Wnt inhibition and ACD systematically.

An intriguing observation in the present study is that a small molecule induces ACD by promoting β-catenin turnover in SW480 cells. In addition to its well-defined roles in cell adhesion and Wnt signaling, β-catenin is also critical in the microtubule array organization, bipolar mitotic spindle establishment, and centrosome separation during mitosis and cell division (38, 39). It would be reasonable to speculate that the decrease in β-catenin alters its behavior in spindle orientation and consequently leads to ACD. A unique advantage of axitinib as an ACD inducer could be that symmetrically dividing cells are more susceptible to axitinib than asymmetrically dividing cells. Cancer cells divide symmetrically to achieve uncontrolled growth, whereas most normal ASCs divide asymmetrically to maintain tissue homeostasis; this difference provides an opportunity for axitinib to target tumors selectively, with less effect on adult tissue homeostasis. For normal ASCs dividing symmetrically in a neutral drift process, the axitinib-mediated switch from SCD to ACD might allow the ASCs to maintain the stem-cell pool continuously by ACD. However, ASCs will be affected by axitinib if SCD is required to expand the stem-cell pool following injury or disease (4, 40), as shown by the inhibited tailfin regrowth in adult zebrafish (Fig. 1*D*).

The human SHPRH gene is located in the chromosomal region 6q24; the observed loss of heterozygosity in a number of cancer types, including skin, prostate, ovarian, breast, cervical, pancreas, and liver, suggests a suppressor role for SHPRH in cancer development and progression (41). The tumor suppressor role of SHPRH is further supported by the depletion of nuclear β-catenin in cancer cells overexpressing SHPRH. In addition, our data show that SHPRH protein is stabilized by axitinib in cancer cells. It would be interesting to assess whether the mechanism is direct or indirect, e.g., whether binding of axitinib changes the interaction of SHPRH and other proteins that might be required for SHPRH modification and turnover. Because SHPRH is a nuclear ubiquitin ligase, axitinib regulates SHPRH and therefore blocks Wnt/β-catenin signaling at the end point of the pathway and would be effective against oncogenic Wnt/β-catenin signaling independent of the mutant genes.

Materials and Methods

Wnt ACD Assay. Cells containing 7TGC or 7TC reporter were synchronized at the G1/S phase by double thymidine block (18 h exposure, 9 h release, and 15 h exposure) and were plated singly in new plates. DMSO or axitinib (5 μM) was added immediately after seeding; 16 h later the images were captured by BioTek Gen5 version 2.06 software, and the intensity of TCF-GFP or TCF-mCherry in paired cells was quantified using the histogram tool of Photoshop software. Wnt signaling was considered to be unequal when paired cells had intensity ratio higher than 2.

***Apc*$^{min/+}$ Mice Study.** C57BL/6-*Apc*$^{Min/+}$ mice were obtained from the Model Animal Research Center of Nanjing University, Nanjing, China. Mice were housed and fed a standard rodent diet at the Animal Facility of the Second Military Medical University, Shanghai, China in compliance with the guidelines of the institutional Animal Care and Use Committee. After 1 wk of acclimation, 10 *Apc*$^{Min/+}$ male mice (7 wk of age) were randomly divided into two groups with similar average weight. Mice were administered vehicle control (0.5% carboxymethylcellulose/H_2O·HCl, pH 2–3) or axitinib at 50 mg/kg by oral gavage daily for five consecutive weeks. The mice were weighed weekly and monitored daily for any signs of illness. The mice were killed on the last day of the treatment. The small intestines were dissected, washed in PBS, fixed in 4% (vol/vol) PBS-buffered formaldehyde, and embedded in paraffin using standard procedures.

DARTS Assay. The DARTS assay was performed according to the protocol previously described (25). To prepare DARTS samples for mass spectrometry analysis, 1×10^7 SW480 cells were lysed in 2.4 mL M-PER (Pierce, 78501) buffer containing freshly added protease inhibitors. After centrifugation and the addition of 10× TNC buffer [500 mM Tris·HCl (pH 8.0), 500 mM NaCl, 100 mM $CaCl_2$], lysates were equally divided between two tubes for incubation for 1 h at room temperature with 20 μL DMSO or 10 mM axitinib. Incubated samples were digested with 4.2 mg/mL pronase at room temperature for 30 min. Digestion was stopped by adding protease inhibitors (11836153001; Roche), and samples were stored at −80 °C for proteomics analysis.

Statistical Analysis. For mice and adult zebrafish experiments, no statistical methods were used to predetermine sample size, but animals in each group were selected randomly. The sample size (*n*) of each experiment is indicated in the relevant figure legends. All experiments using cultured cells and zebrafish embryos were repeated at least with three biological replicates. A two-tailed Student's *t* test was performed to evaluate the statistical difference for all pairwise comparisons. Fisher's exact test was used to analyze the proportions or calculate the probability of overlap between gene lists. Pooled data are represented as the mean ± SD of the replicated experiments. *P* values are indicated in figure legends, and differences were considered significant at $*P \leq 0.05$ and $**P \leq 0.01$. In our observations, all measured data were normally distributed, and the variance was similar between the groups that were statistically compared.

ACKNOWLEDGMENTS. We thank Hua My Hoang for DNA microarray profiling; Marianne Eidsheim for immunohistochemistry; Marianne Enger and the Molecular Imaging Centre at the University of Bergen for flow cytometry; Tohru Ishitani and Akiko Ishioka for the Tcf/Lef-miniP:dGFP line; Alex Greenhough for the β-catenin-ΔLIR vector; and Karlene Cimprich for the GFP-SHPRH vector. This project received funding from Einar Galtung Døsvig, Espen Galtung Døsvig, Jan Einar Greve, Thorstein Selvik, Kåre Rommetveit, Trond Mohn, Herman Friele, Bjarne Rieber, and from the Tordis and Fritz C. Rieber's Foundation; Bergen Medical Research Foundation; Helse Vest Grants 911778, 911626, 911747, and 912062; Centre for Cancer Biomarkers; Research Council of Norway Grant 223250/F50; South-Eastern Norway Regional Health Authority Grant 2015095 (Regional Core Facility for Structural Biology); Norwegian Cancer Society Grant 803148; and Natural Science Foundation of China Grant 81230090.

1. Kahn M (2014) Can we safely target the WNT pathway? *Nat Rev Drug Discov* 13(7):513–532.
2. Clevers H, Nusse R (2012) Wnt/β-catenin signaling and disease. *Cell* 149(6):1192–1205.
3. Lenz HJ, Kahn M (2014) Safely targeting cancer stem cells via selective catenin coactivator antagonism. *Cancer Sci* 105(9):1087–1092.
4. Morrison SJ, Kimble J (2006) Asymmetric and symmetric stem-cell divisions in development and cancer. *Nature* 441(7097):1068–1074.
5. Bajaj J, Zimdahl B, Reya T (2015) Fearful symmetry: Subversion of asymmetric division in cancer development and progression. *Cancer Res* 75(5):792–797.
6. Quyn AJ, et al. (2010) Spindle orientation bias in gut epithelial stem cell compartments is lost in precancerous tissue. *Cell Stem Cell* 6(2):175–181.
7. Sato N, Meijer L, Skaltsounis L, Greengard P, Brivanlou AH (2004) Maintenance of pluripotency in human and mouse embryonic stem cells through activation of Wnt signaling by a pharmacological GSK-3-specific inhibitor. *Nat Med* 10(1):55–63.
8. Fuerer C, Nusse R (2010) Lentiviral vectors to probe and manipulate the Wnt signaling pathway. *PLoS One* 5(2):e9370.
9. van de Water S, et al. (2001) Ectopic Wnt signal determines the eyeless phenotype of zebrafish masterblind mutant. *Development* 128(20):3877–3888.
10. Shimizu N, Kawakami K, Ishitani T (2012) Visualization and exploration of Tcf/Lef function using a highly responsive Wnt/β-catenin signaling-reporter transgenic zebrafish. *Dev Biol* 370(1):71–85.
11. Buckles GR, Thorpe CJ, Ramel MC, Lekven AC (2004) Combinatorial Wnt control of zebrafish midbrain-hindbrain boundary formation. *Mech Dev* 121(5):437–447.
12. Nagayoshi S, et al. (2008) Insertional mutagenesis by the Tol2 transposon-mediated enhancer trap approach generated mutations in two developmental genes: Tcf7 and synembryn-like. *Development* 135(1):159–169.
13. Watanabe K, et al. (2014) Integrative ChIP-seq/microarray analysis identifies a CTNNB1 target signature enriched in intestinal stem cells and colon cancer. *PLoS One* 9(3):e92317.
14. Huels DJ, et al. (2015) E-cadherin can limit the transforming properties of activating β-catenin mutations. *EMBO J* 34(18):2321–2333.
15. van der Flier LG, Clevers H (2009) Stem cells, self-renewal, and differentiation in the intestinal epithelium. *Annu Rev Physiol* 71:241–260.
16. Stoick-Cooper CL, et al. (2007) Distinct Wnt signaling pathways have opposing roles in appendage regeneration. *Development* 134(3):479–489.
17. Beck B, Blanpain C (2013) Unravelling cancer stem cell potential. *Nat Rev Cancer* 13(10):727–738.
18. Conboy MJ, Karasov AO, Rando TA (2007) High incidence of non-random template strand segregation and asymmetric fate determination in dividing stem cells and their progeny. *PLoS Biol* 5(5):e102.
19. Caussinus E, Gonzalez C (2005) Induction of tumor growth by altered stem-cell asymmetric division in Drosophila melanogaster. *Nat Genet* 37(10):1125–1129.
20. Sugiarto S, et al. (2011) Asymmetry-defective oligodendrocyte progenitors are glioma precursors. *Cancer Cell* 20(3):328–340.
21. Li VS, et al. (2012) Wnt signaling through inhibition of β-catenin degradation in an intact Axin1 complex. *Cell* 149(6):1245–1256.
22. Harada N, et al. (1999) Intestinal polyposis in mice with a dominant stable mutation of the beta-catenin gene. *EMBO J* 18(21):5931–5942.
23. Chen B, et al. (2009) Small molecule-mediated disruption of Wnt-dependent signaling in tissue regeneration and cancer. *Nat Chem Biol* 5(2):100–107.
24. Huang SM, et al. (2009) Tankyrase inhibition stabilizes axin and antagonizes Wnt signalling. *Nature* 461(7264):614–620.
25. Petherick KJ, et al. (2013) Autolysosomal β-catenin degradation regulates Wnt-autophagy-p62 crosstalk. *EMBO J* 32(13):1903–1916.
26. Xue J, et al. (2015) Tumour suppressor TRIM33 targets nuclear β-catenin degradation. *Nat Commun* 6:6156.
27. Hu-Lowe DD, et al. (2008) Nonclinical antiangiogenesis and antitumor activities of axitinib (AG-013736), an oral, potent, and selective inhibitor of vascular endothelial growth factor receptor tyrosine kinases 1, 2, 3. *Clin Cancer Res* 14(22):7272–7283.
28. Naik S, Dothager RS, Marasa J, Lewis CL, Piwnica-Worms D (2009) Vascular Endothelial Growth Factor Receptor-1 Is Synthetic Lethal to Aberrant beta-Catenin Activation in Colon Cancer. *Clin Cancer Res* 15(24):7529–7537.
29. Bayliss PE, et al. (2006) Chemical modulation of receptor signaling inhibits regenerative angiogenesis in adult zebrafish. *Nat Chem Biol* 2(5):265–273.
30. Lomenick B, et al. (2009) Target identification using drug affinity responsive target stability (DARTS). *Proc Natl Acad Sci USA* 106(51):21984–21989.
31. Unk I, et al. (2006) Human SHPRH is a ubiquitin ligase for Mms2-Ubc13-dependent polyubiquitylation of proliferating cell nuclear antigen. *Proc Natl Acad Sci USA* 103(48):18107–18112.
32. Wienken CJ, Baaske P, Rothbauer U, Braun D, Duhr S (2010) Protein-binding assays in biological liquids using microscale thermophoresis. *Nat Commun* 1:100.
33. Khavrutskii L, et al. (2013) Protein purification-free method of binding affinity determination by microscale thermophoresis. *J Vis Exp* (78):e50541.
34. Martinez Molina D, et al. (2013) Monitoring drug target engagement in cells and tissues using the cellular thermal shift assay. *Science* 341(6141):84–87.
35. Motegi A, et al. (2006) Human SHPRH suppresses genomic instability through proliferating cell nuclear antigen polyubiquitination. *J Cell Biol* 175(5):703–708.
36. Pemovska T, et al. (2015) Axitinib effectively inhibits BCR-ABL1(T315I) with a distinct binding conformation. *Nature* 519(7541):102–105.
37. Hopkins AL (2008) Network pharmacology: The next paradigm in drug discovery. *Nat Chem Biol* 4(11):682–690.
38. Ligon LA, Karki S, Tokito M, Holzbaur ELF (2001) Dynein binds to beta-catenin and may tether microtubules at adherens junctions. *Nat Cell Biol* 3(10):913–917.
39. Kaplan DD, Meigs TE, Kelly P, Casey PJ (2004) Identification of a role for beta-catenin in the establishment of a bipolar mitotic spindle. *J Biol Chem* 279(12):10829–10832.
40. Piccin D, Morshead CM (2011) Wnt signaling regulates symmetry of division of neural stem cells in the adult brain and in response to injury. *Stem Cells* 29(3):528–538.
41. Sood R, et al. (2003) Cloning and characterization of a novel gene, SHPRH, encoding a conserved putative protein with SNF2/helicase and PHD-finger domains from the 6q24 region. *Genomics* 82(2):153–161.
42. Ke XS, et al. (2008) Epithelial to mesenchymal transition of a primary prostate cell line with switches of cell adhesion modules but without malignant transformation. *PLoS One* 3(10):e3368.
43. Qu Y, et al. (2013) Generation of prostate tumor-initiating cells is associated with elevation of reactive oxygen species and IL-6/STAT3 signaling. *Cancer Res* 73(23):7090–7100.
44. Major MB, et al. (2008) New regulators of Wnt/beta-catenin signaling revealed by integrative molecular screening. *Sci Signal* 1(45):ra12.
45. Hatzis P, et al. (2008) Genome-wide pattern of TCF7L2/TCF4 chromatin occupancy in colorectal cancer cells. *Mol Cell Biol* 28(8):2732–2744.
46. Su AI, et al. (2004) A gene atlas of the mouse and human protein-encoding transcriptomes. *Proc Natl Acad Sci USA* 101(16):6062–6067.
47. Komashko VM, et al. (2008) Using ChIP-chip technology to reveal common principles of transcriptional repression in normal and cancer cells. *Genome Res* 18(4):521–532.